Towards More Reliable Renewable Power Systems - Thermal Performance Evaluation of DC/DC Boost Converters Switching Devices

C. Batunlu, A. Albarbar
Engineering and Materials Research Centre,
School of Engineering, Manchester Metropolitan University, Manchester, UK

Article Info	ABSTRACT
	Power electronic converters (PECs) are one of the most important elements within renewable power generation systems. The reliability of switching elements of PECs is still below expectations and is a major contributor to the downtime of renewable power generation systems. Conventional technology based elements such as Silicon Insulated Gate Bipolar Transistors (IGBTs) operate as switching components in PECs. Recent topological improvements have led to new devices called Silicon Carbide (SiC) MOSFETs which, are also being used as switching elements for PECs. This paper presents detailed investigations into the performance of those switching devices with a focus on their reliability and thermal characteristics. Namely, trench gate NPT, FS IGBT topologies and SiC MOSFET are firstly modelled using 3-D multi-physics finite element modelling to gain clear understanding of their thermal behaviour. Subsequently, modelling outcomes are verified by using those devices as switching elements in operational boost converters. The purposely-developed test setups are utilised to critically assess the performances of those switching devices under different loading and environmental conditions. In general, SiC device was found to exhibit about 20 °C less in its operating temperature and therefore expected to offer more reliable switching element.

Corresponding Author:

Alhussein Albarbar,
School of Engineering,
Manchester Metropolitan University,
Manchester, M1 5GD, UK.
Email: a.albarbar@mmu.ac.uk

1. INTRODUCTION

Insulated gate bipolar transistors (IGBTs) are one of the most commonly used switching elements of power electronic converters (PECs) in various applications such as motor drives [1], traction [2], UPS [3], hybrid [4] and renewable power systems [5]. Thanks to recent developments, operating voltage of this silicon, Si, structured device is up to 6.5 kV with switching frequency range 1-100 kHz [6]. As it is well defined in literature [7], during operation, switching and conduction losses within these devices are the major contributor of the temperature fluctuations. Thermal stress occurs due to these losses which leading to degradation and eventual failures. Especially, IGBT chip thickness reduction process for improving dynamic electrical properties caused higher thermal resistances. To overcome these challenges, the recent *trend* is *moving* towards different technologies such as transistors built from Silicon Carbide (SiC) and Galium Nitride (GaN) [8],[9]. Physical material specification differences among these technologies and their superior properties can be seen in Table 1. Recent studies are taking place for fabrication of high performance SiC MOSFET which reduces power losses especially at high carrier frequencies [10]. Analytical formulation of
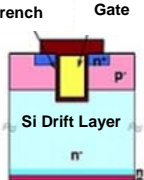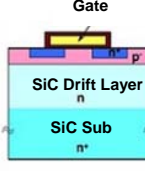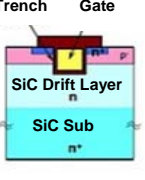
injection capability of SiC device has been proposed by Lee and Huang [11]. Degradation characteristics and features of SiC devices have been presented in [12]-[13]. It has been investigated that SiC structured transistors can be operated at higher switching and temperature capacities [14]-[15].

Table 1: Physical characteristic differences among semiconductor technologies [14]-[16]

Properties	Si	GaAs	GaN	4H-SiC	6H-SiC	Unit
Crystal Structure	Diamond	Zincblende	Hexagonal	Hexagonal	Hexagonal	-
Bandgap (E_G)	1.10	1.43	3.5	3.26	3	eV
Electron Mobility (μ_n)	1400	8500	1250	900	380	cm^2/V_s
Hole Mobility (μ_p)	600	400	200	100	80	cm^2/V_s
Dielectric Constant (ε_S)	11.8	12.8	9.5	10.1	9.66	-
Saturation Drift Velocity (v_s)	1×10^7	2×10^7	2.7×10^7	2.7×10^7	2×10^7	cm/s
Breakdown Field (E_B)	0.3×10^6	0.4×10^6	3×10^6	3×10^6	3×10^6	V/cm
Thermal Conductivity (k)	1.5	0.5	1.3	4.9	4.9	W/cm°C
Melting Point	1420	1283	2500	2830	2830	°C

Conventional IGBTs can be operated at higher current densities with lower frequency while the MOSFETs have better efficiency at higher operating frequencies over 100 kHz**.** In contrast, recently developed SiC MOSFETs have much smaller channel mobility compared to conventional ones [17]-[18] which reflects increase in total cost. On the other hand, the thermal conductivity of SiC is much higher than that for silicon [18], so dissipated heat can easily be removed from the device. Regardless promising material properties of SiC, Si devices can still be more reliable and economically efficient based on the current rating and switching frequency of a specific application [19]. Topological physical differences among Si IGBT and SiC Planar and Trench Gate MOSFETs can be seen in Table 2. In an effort to overcome downsides of conventional planar gate IGBT technologies, such as negative temperature coefficient of Punch-Through (PT) and increased conduction losses, due to the thicker substrate of Non-Punch Through (NPT) devices, trench gate technology has been developed [20],[21]. Reduced diameter of the gate provides enhancement of charge injection, reduced tail current at turn off, as well as reduced conduction and switching losses [22],[23]. Since the voltage drop over the channel is inversly proportional to the channel width and proportional to the length of the channel, lower conduction losses were achived by shortening the channel [24]. For instance, trench gate devices can provide around 30% power dissipation deduction for 600 V IGBTs, typically optimized at 20 kHz switching frequency, in DC-to-AC inverter applications [25],[26]. Further improvements were achieved by a field stop (FS) region which is added to thin-wafer NPT device. This layer stops the electric field and allows high breakdown voltage through thinner wafer. It results in faster switching capabilities, higher current density, as well as lower saturation collector to emitter voltage and 40% reduction in the conduction losses. Multi trench NPT and FS based IGBTs can be seen in Figure 1. In literature, electro thermal physics-based model for the FS was developed by Kang et al. [25].

Table 2. Si IGBT and SiC MOSFET technologies

Material	Silicon	SiC	SiC
Physical Structure			
Technology	IGBT	MOSFET	
Gate	Trench	Planar	Trench

Practical studies proposed by Forsyth et al. [26] to parameterise a physical IGBT model, for three generations of IGBT, using double-pulse switching test, at temperatures extending down to 50°K.. Effect of different parasitic circuit characteristics of NPT and FS topologies have also been presented by Bakran et al. [27]. More IGBT cells are used with thinner silicon for even lower on-state voltage and improved switching characteristics. Higher switching speed leading to lower switching losses but causes EMI whilst keeping the turn on losses low due to gradual change in voltage with respect to current [28]. Thermal profile improvement and monitoring is one essential reason of technological improvements. Comparison of junction temperature evaluations in IGBT modules [29],[30] as well as the measurement and modelling of power

electronic devices at cryogenic temperatures have been studied in [31]. Characterization of high-voltage IGBT module degradations under PWM power cycling test at high ambient temperature has also been assessed in [32]. Yet, no rigorous investigation has been carried out to assess the effects of design and construction techniques on thermal behaviour under different operating and environmental conditions.
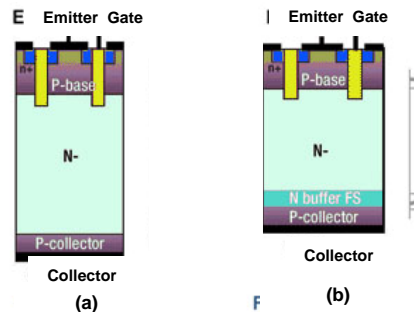

Figure 1. (a) Trench NPT (b) FS within Trench IGBT

In this work, thermal characteristics of trench gate IGBTs and recently developed SiC based MOSFET were compared under different operating and environmental conditions. In Section 2, experimental setup and real time temperature monitoring progress of DC/DC Boost converters, integration within dSPACE system are demonstrated. Electro thermal model of sample Si IGBT and SiC MOSFET devices are described in Simulink and 3D FE analysis in Section 3. The results are presented in Section 4, where thermal behaviour comparison of stated technologies is shown within different environmental conditions. Conclusions are depicted in final section.

2.   BOOST CONVERTER DESIGN AND THERMAL ANALYSIS

DC-DC converters are widely used in a number of applications, such as power factor correction [33], fuel cell [34] applications, maximum power point tracking of solar and wind energy systems [35],[36]. Figure 2 shows schematic of DC/DC boost converter.
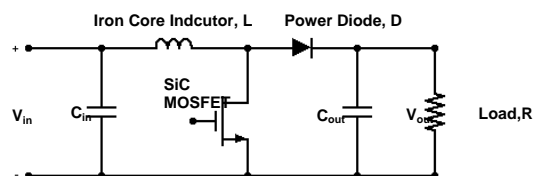

Figure 2. Boost Converter with SiC MOSFET

Two trench gate Si NPT and FS IGBTs and a SiC based MOSFET semiconductor devices was selected. The characteristics of selected components are shown in Table 3. Three boost converters were built by using these devices along with identical blocking and storing elements for thermal comparison purpose.

Table 3. Si IGBTs and SiC MOSFET specifications

IGBT (1)	IGBT (2)	MOSFET	Unit
NPT-Si-Trench	FS-Si-Trench	SiC-Planar	-
Cost: 1.00	Cost: 1.19	Cost: 11.52	£
V_{CEs}: 600	V_{CEs}: 600	V_{DSs}: 1200	V
$I_{C\,(T=25C)}$: 25	$I_{C\,(T=25C)}$: 20	$I_{D\,(T=25C)}$: 24	A
$I_{C\,(T=100C)}$: 15	$I_{C\,(T=100C)}$: 10	$I_{D\,(T=100C)}$: 10	A
C_{ies}: 1950	C_{ies}: 551	C_{iis}: 667	pF
C_{oes}: 70	C_{oes}: 40	C_{oss}: 27	pF
C_{res}: 42	C_{res}: 17	C_{rss}: 5	pF
Q_g: 88	Q_g: 62	Q_g: 36	nC
$t_{d(on)\,(T=25C)}$: 65	$t_{d(on)\,(T=25C)}$: 12	$t_{d(on)\,(T=25C)}$: 19	ns
t_r: 28	t_r: 8	t_r: 19	ns
$t_{d(off)}$: 170	$t_{d(off)}$: 215	$t_{d(off)}$: 47	ns
t_f: 140	t_f: 38	t_f: 29	ns
$E_{on\,(T=25C)}$: 0.55	$E_{on\,(T=25C)}$: 0.16	$E_{on\,(T=25C)}$: 0.057	mJ
$E_{off\,(T=25C)}$: 0.35	$E_{off\,(T=25C)}$: 0.27	$E_{off\,(T=25C)}$: 0.02	mJ
$P_{loss(T=25C)}$: 117	$P_{loss(T=25C)}$: 110	$P_{loss(T=25C)}$: 108	W

Wide range of load power cycling as well as different ambient temperature and switching frequency characteristics have been applied for investigating thermal behaviour and efficiency of these devices and to verify the proposed Finite Element Modelling (FEM) approach based on real power loss data processed through dSPACE Real Time Interface (RTI). The experimental test rig is shown in Figure 3(a).
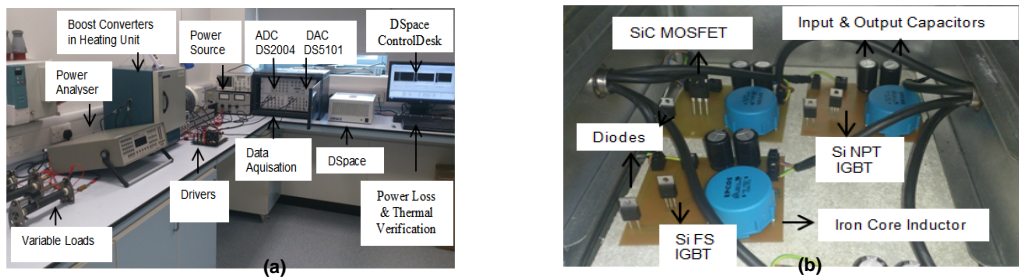

Figure 3. (a) Experimental set-up, (b) Boost converters in temperature controlled chamber (TCC)

Converter Parameter specifications are listed in Table 4. An iron-core type inductor was used to decrease saturation of current flow. A fast recovery diode was used for Si and SiC based boost converter to limit the comparison criteria only for switching devices. Switching frequencies between 5 to 150 kHz was applied in separate test conditions where duty cycle was always set as 50 %. Boost converters were placed in heating unit as shown in Figure 3(b).

Table 4. Boost Converter parameter specifications

Element	V_{in}	IGBTs	MOSFET	Diode	S. Freq.	Duty	Inductor, L	C_{in}, C_{out}
Values	5-70 V	600/15A	1200/15A	300/20A	5-150 kHz	50%	1mH	82µF/450V

The gate signals for each IGBTs and MOSFET were generated using dSPACE real time system with DS5101 digital to analogue converter card. Due to the critical gate requirements, HCPL 4503 opt coupler was used to isolate low power switching signal and TD351 IGBT/MOSFET driver was adopted for supplying efficient gate signal power. Hall-effect based ACS712 linear current sensors were used to monitor collector current, I_c, and to insert power loss model in RTI through DS2004ADC as well as the collector to emitter voltage, V_{ce}. Total energy losses are defined as function of I_{ce}, V_{ce} and device temperature in look up tables. To produce real time power loss profile, switching losses are triggered in nanoseconds during current/voltage switching process and are multiplied by the switching frequency. Since power loss occurred on device under test is highly depend on the operation temperature, analytical loss calculations show significant inaccuracies [37]. By using real time loss profile, accuracy of the electro thermal model was improved in this paper. Heat generation of freewheeling diodes is negligible [38] therefore, they were not considered in this study.
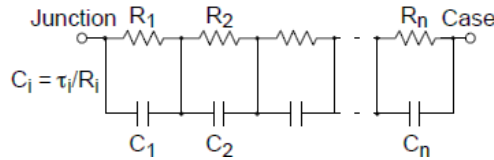
Figure 4. Foster thermal network

Total power losses were integrated as input for thermal model block. In this block, thermal resistance, R_{th} and capacitance, $C_{th,}$ for each individual of Foster equivalent thermal network, see Figure 4, were extracted by curve fitting using least square method. Implementation of real time thermal monitoring in DSPACE is shown in Figure 5. The equivalence of Foster thermal network is defined in eqn. 1 as:

$$T_m(s) = \sum_{k=1}^{N} \frac{1/Cth_n}{s+1/\tau_n} P_n(s)$$
(1)

where P is the initial heat source. Temperature, T, of each layer was represented for heating source. By applying Forward Rectangular Euler's rule, thermal equation in z-domain is:

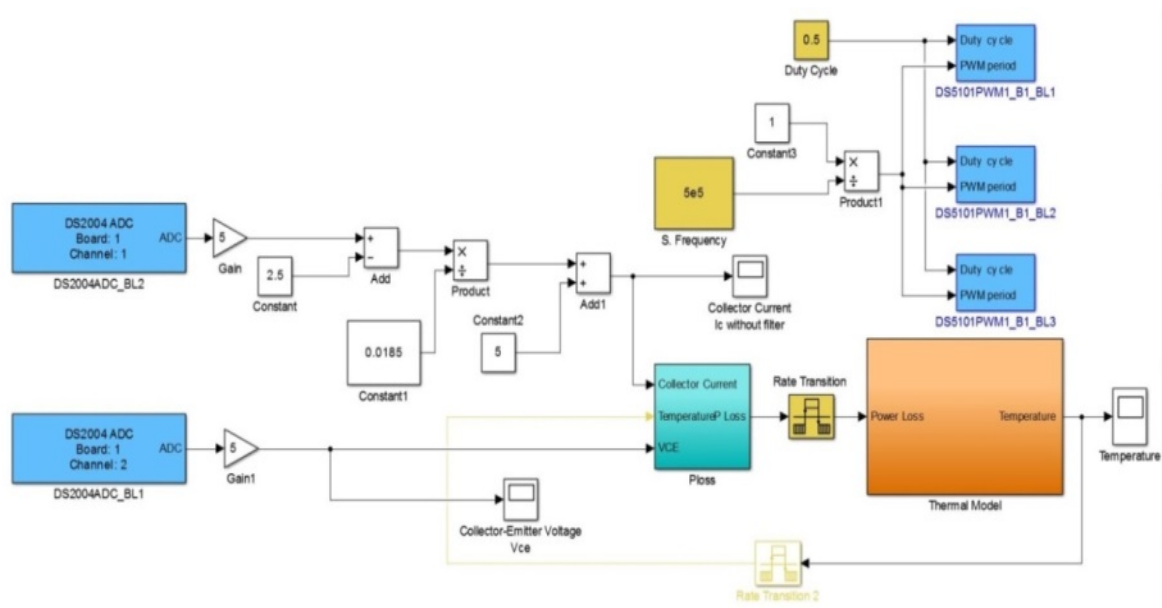$$\Delta T = \frac{P_i}{C_{th}} \frac{1}{z-1} - \frac{\Delta T}{R_{th}C_{th}} \frac{1}{z-1}$$
(2)

Figure 5. Real Time Implementation of Electro thermal Model in dSPACE

3.   FINITE ELEMENT MODELLING

Finite element model of the both Si IGBT and SiC MOSFET have been completed in a compact thermal modelling approach. However for increasing the accuracy, recorded power loss data by RTI of electro thermal experiment defined above was directly applied to the silicon die chip of the IGBTs in FE analysis. Heat distribution through each material was generated using Eqn. 3:

$$\frac{\partial^2 T}{\partial x^2} + \frac{\partial^2 T}{\partial y^2} + \frac{\partial^2 T}{\partial z^2} + \frac{q}{k} = \frac{\rho.c}{k} \frac{\partial T}{\partial t}$$
(3)

where T is the temperature, k is the thermal conductivity, c is specific heat capacity, ρ is the density and q is the rate of generation of energy per unit volume.
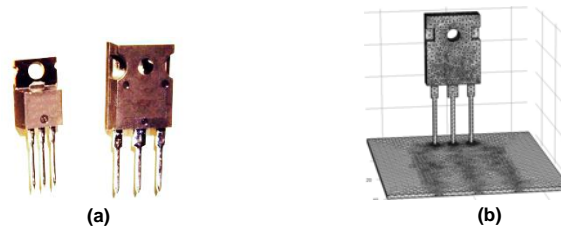
Figure 6. (a) TO-220 (left) and TO-247 (right) Packages, (b) View of FE model for TO-247

As shown in Figure 6(a), TO220 package constructed for IGBTs is different than the TO247 for SiC MOSFET in terms of dimensions. Chip size of MOSFET is almost two times greater compared to both FS and NPT IGBTs where FS one's is half of NPT's. Mesh view of model can be seen in Figure 6(b). The total number of tetrahedral elements was 57082. Mesh refinement was completed by the scale factor of two especially for the solder layers. Temperature depended material propoerties, are presented in Table 5, are defined as dynamic arguments where for cooling boundary condition, the natural convection, h, in model was assigned as 5 W/m^2K.

Table 5. Material Properties

Layer	Physical Properties at 25 °C		
	p (kg/m³)	k(W/mK)	c(J/(kgK)
T0220 Silicon Chip	2330	153	703
T0247 SiC Chip	3216	490	690
Copper	8850	398	380
Gold	19300	318	129
PLCC	900	0.2	1700
Steel Alloy	7850	54	477
Mica	2883	0.71	500
Aluminium	3010	180	741
Grease	-	2	-

4. RESULT AND DISCUSSIONS
4.1. Thermal measurement and RTI model verification
Thermal model was built upon operating switching elements in continuous conduction mode with a constant gate voltage. Device temperatures had been monitored by thermal imaging and recorded in 5 seconds intervals. Based on obtained transient temperature profile, thermal impedance for each component have been interpolated as in eqn. 2 and shown in Table 6.

Table 6. Thermal impedance characteristics

Device LUT	Thermal Capacitances			Thermal Resistances		
	$C_{th,1}$	$C_{th,2}$	$C_{th,3}$	$R_{th,1}$	$R_{th,2}$	$R_{th,3}$
FS	0.22	0.02	0.0013	0.2911	0.409	0.5008
NPT	0.28	0.018	0.0014	0.2911	0.4	0.5019
SiC MOSFET	0.51	0.050	0.002	0.153	0.14	0.4003
Device FE						
FS	0.2	0.0118	0.0016	0.28	0.481	0.509
NPT	0.21	0.022	0.0016	0.27	0.401	0.505
SiC MOSFET	0.53	0.06	0.0023	0.149	0.16	0.412

SiC MOSFET has double thermal capacitance and half of resistance of both FS and NPT IGBTs which leading to lower thermal fluctuations and amplitude. Figure 7(a) shows thermal images of converters at 25°C ambient temperature when input voltage of boost converter is 5V, switching frequency is 20 kHz and current passes each device is 0.5A.
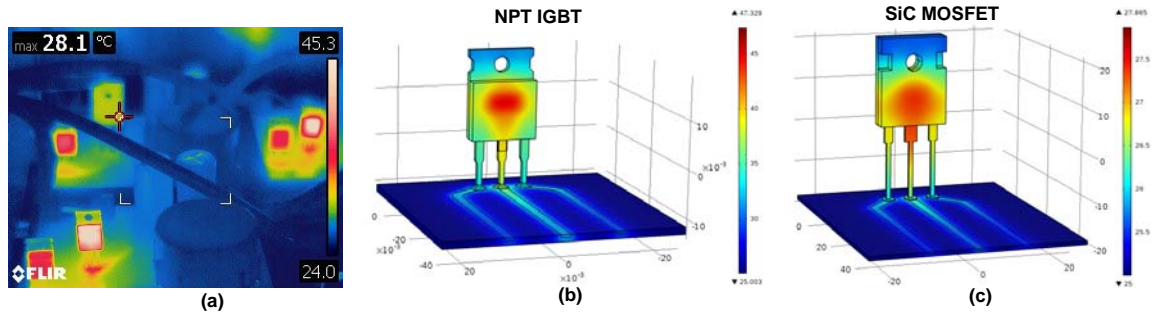
Figure 7. a) Boost Converters in heating unit, (b) NPT IGBT and (c) SiC MOSFET Thermal FE models

FE model solutions of defined devices can be seen in Figure 7(b) for NPT IGBT and Figure 7(c) for MOSFET. Good agreement has been obtained in terms of steady state temperature and total heat distribution over each device. It is distributed through collector in both results. The NPT IGBT has the highest temperature profile while the SiC MOSFET was subjected to 50% of the NPT's as 45.3°C and 28.1°C, respectively. After implementing electro-thermal model with the addition of thermal models described above the device temperatures were monitored in dSPACE Control Desk, based on the processed device current and voltages. The associated total power loss data for each device have been stored during this test and applied to each related topological chip in FE models described in Section 2.
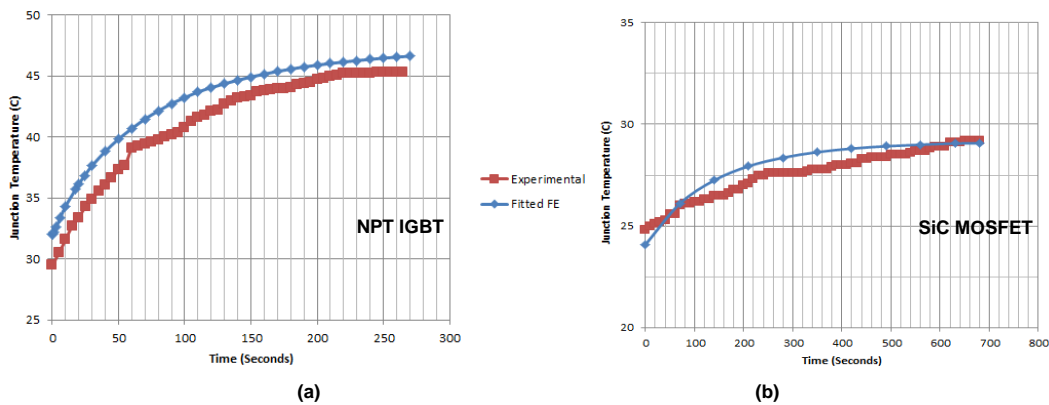

Figure 8. Transient temperature comparison for (a) Si NPT IGBT (b) SiC MOSFET FE models

Approximately 2°C difference was measured for NPT IGBT where this is less than 1°C for MOSFET. Transient temperature results for both device are shown in Figure 8 (a) and (b). It can be clearly seen that the SiC MOSFET has heat higher heat capacity since it reaches the final temperature at around 800 s whilst this much shorter for NPT. The accuracy of the proposed FE model approach can still be validated based on transient analysis.

4.2. Ambient temperature and switching frequency effect tests without heat sink
Two sets of experimental tests were performed. First the devices were operated without heat sinks and, current passes through IGBTs and SiC MOSFET was set as 0.5A by variable resistors. Converters were operated in temperature controlled chamber (TCC) simultaneously for a set of switching frequencies between 10-150 kHz and the ambient temperature was changed in steps of 5°C from 25 to 50 °C. Temperature of each switching device was monitored by FLIR T440 thermal camera with frame rate 60Hz and a thermal resolution of 76,800 pixels and recorded for each frequency at different ambient temperatures.
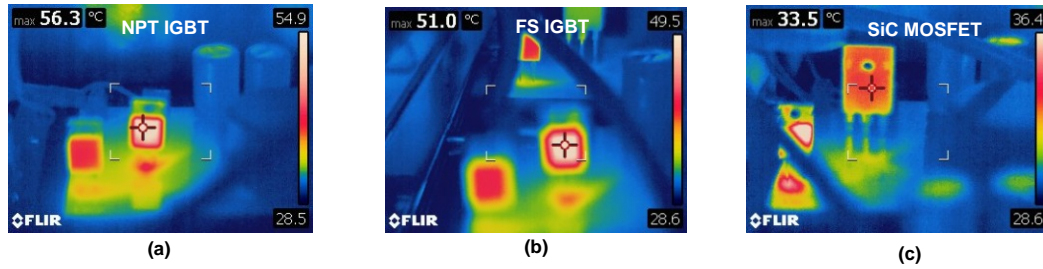
Figure 9. Thermal camera view (a) NPT IGBT, (b) FS IGBT, (c) MOSFET at 30°C ambient temperature

Figure 9 shows the boost PECs at 35°C ambient temperature when the switching frequency of boost converters was 50 kHz. FS IGBT temperature was approximately 5°C less than NPT's while the SiC MOSFET showed better thermal performance compare to both Si IGBT devices with temperature of 33.5 °C.
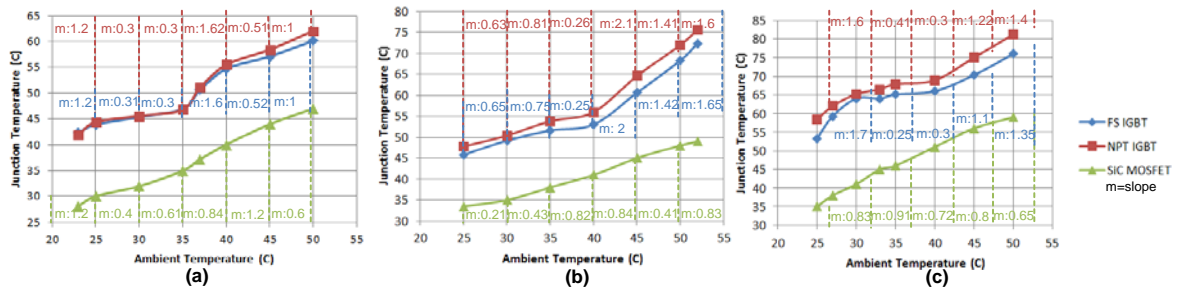

Figure 10. Ambient temperature effect on device temperature at (a) 20 kHz, (b) 50 kHz, (c) 150 kHz

For both Si IGBTs, effect of ambient temperature was observed as lower at 35-40°C regions as shown in Figure 10. Beyond this point, temperature trend shows higher slope until 55°C ambient. MOSFET temperature showed more linear incline with respect to ambient temperature and can be commented as less dependent to this parameter especially at higher switching frequencies. Moreover, temperature between both IGBTs increase as the frequency inclines due to the higher switching losses of NPT device caused by longer tail current.
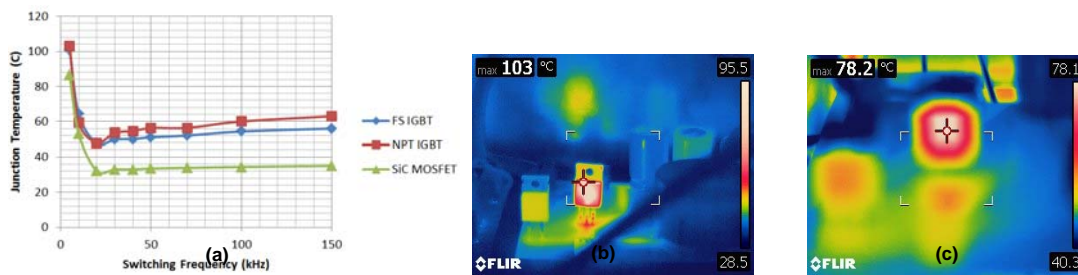

Figure 11. (a) Switching Frequency vs. device temperature, (b) NPT IGBT at 103°C and (c) at 78.2°C

The effect of switching frequency is further analysed as shown in Figure 11(a) at 30 °C ambient temperature. The conduction losses superior at frequencies lower than 15 kHz for each device and hence the temperature rise can be detected up to i.e. 103 °C for NPT as shown in Figure 11(b). Same device has highest temperature of 78.2 °C when operated at 150 kHz at ambient temperature of 40 °C as seen in Figure 11(c). MOSFET is more preferable at higher frequencies as high as 150 kHz. Compared to both IGBTs its maximum junction temperature is only increased 2°C while this was 11°C for FS and 13°C for NPT IGBTs when the frequcny increased from 20 to 150 kHz.

4.3. Power efficiency and current effect operation with attached heat sinks

Further tests have been employed with higher current ratings when heat sinks are attached to 1 devices. The ambient temperature was kept constant at 25°C and switching frequency of converters was 20 kHz. Boost converters were tested with equal loads, simultaneously. Therefore switching devices were subjected slightly different current ratings based off efficiency of individual converter compared to the analysis in Section 4.2.
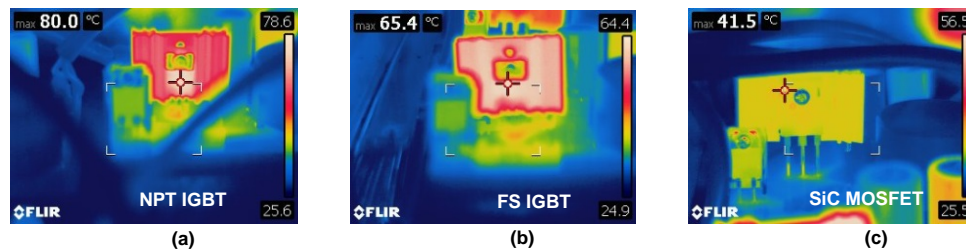

Figure 12. Thermal camera view (a) NPT IGBT, (b) FS IGBT, (c) MOSFET at 25°C ambient temperature

Steady state temperature distributions are shown in Figure 12 shows at 2A load current. The temperature difference among each device is approximately as high as 15°C where the NPT has highest temperature of 80°C and the SiC MOSFET is operated at 41.5°C. The highest current rating of each device is 15 A and due to laboratory limitation the load current was increased up to 5A. It was found that thermal performance of SiC device decreases as the current rating inclines. The SiC MOSFET is superior Si IGBT devices at higher frequencies. However, Si IGBTs shows more consistent thermal profile at higher current ratings especially above 2A as seen in Figure 13(a). This range can change for different power rating devices. In this study, for accurate comparison, current capacity and total power loss of each device have been selected as same. FE model results for FS IGBT and MOSFET can also be seen in Figure 13(b) and (c) when heat sinks are attached at the back of both devices via a thermal grease layer, during high current operation. Processed total power loss data by RTI directly applied to chips in FEM. Good accuracy was also obtained especially for T0-247 packaged MOSFET with only 1.5 °C difference compare to experimental result shown in Figure 12(c).
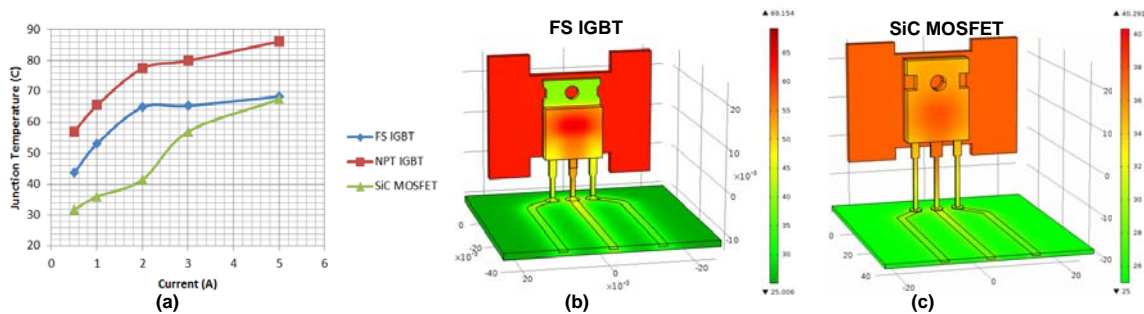

Figure 13. (a) Device temperature vs current (b) FS IGBT and (c) SiC MOSFET Thermal FE models

For FS IGBT, temperature difference is approximately 3.5 °C compared to experimental case due to difference in package type TO-220 and geometrical assumptions on heat sink modelling. As stated before for estimating total power losses and transient temperature, switching transient of each device (on-off state voltage/current) was processed through dSPACE Control Desk into electro thermal models using Simulink are shown in Figure 14.
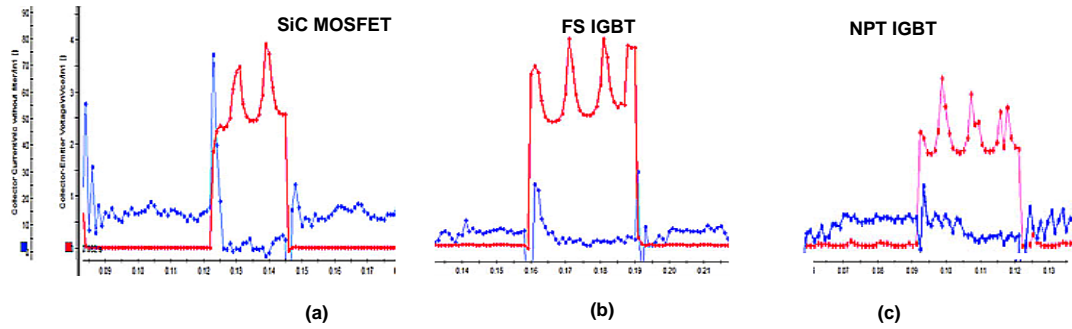
Figure 14. Switching transient of (a) SiC MOSFET, (b) FS IGBT (c) NPT IGBT

As it is seen, SiC device has very little tail current; hence lower switching off losses compared to the both Si IGBTs. This also proves the better thermal performance of MOSFET at higher switching frequencies. On the other hand, NPT IGBT has the highest switching transient time among all devices where the FS technology performance still compatible with SiC MOSFET in terms of thermal performance at higher current ratings. It was also estimated that conduction losses of NPT's increases as the temperature inclines due to positive temperature coefficient. IGBT costs, evaluated in this paper, are one tenth the cost of SiC MOSFET. As indicated previously, production cost of the SiC device is more expensive. Bigger die size of MOSFET compared to IGBTs, which is three times bigger than NPTs', is also one reason for expensive device cost. Depending on the priorities of the design, although IGBT companies offer "higher Vce/lower switching energy device" for high frequency applications, and vice versa for a low frequency applications, MOSFET is still effective at the frequencies above 150 kHz in terms of thermal performance. Below this frequency, both IGBTs, evaluated in this study, can be viable competitor of SiC MOSFET especially at higher current limits of an individual device with the help of their lower conduction loss characteristics.
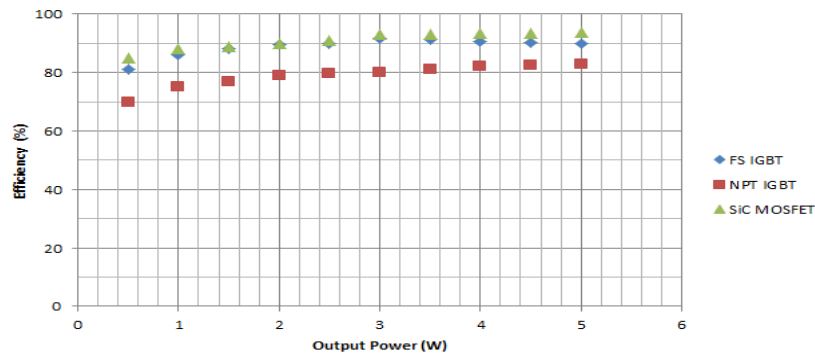

Figure 15. Output power efficiency of Boost Converter among each device

Efficiency of boost converter is shown in Figure 15 when the ambient temperature was kept constant at 30°C and the switching frequency was 20 kHz. Under all loading cases, SiC MOSFET based converter was more efficient than the ones with IGBTs. Compared to the NPT IGBT, it attained 10% better efficiency where it is approximately 2% higher once compared with the FS device. Efficiency of the FS IGBT is very close to the MOSFET performance, however it slightly decreases when the output power is greater than 3.5 W.

5. CONCLUSION

A real time electro thermal monitoring study was presented for SiC MOSFET and Si based IGBT devices within DC/DC boost converter. Finite element model of these semiconductor components were developed as a function of power loss real-time measurements. The study demonstrates good agreement between model outcomes and obtained experimental results under different environmental and operational conditions such as ambient temperature and switching frequency. SiC device was found more thermally stable particularly at frequencies higher than 100 kHz and has approximately 20°C less operating temperature

characteristic compared to the IGBT devices on most of the tested conditions. However, current increase caused temperature inclination at lower frequencies. FS IGBTs performed the best at frequencies between 10-50 kHz, thanks to their lower conduction loss characteristics. In conclusion, SiC device has a better dynamic response since it has a wider band gap and can block higher voltage and reduce drift region widths due to its higher electric field. Lower recovery current characteristic also leading to less switching losses. Si IGBTs can be selected as switching device for boost converters used in wider frequency range applications if cost matters.

REFERENCES

[1] E. Natsheh, AR. Natsheh, A. Albarbar, "Intelligent Controller For Managing Power Flow Within Standalone Hybrid Power Systems", *IET Science, Measurement & Technology*, vol/issue: 7(4), pp. 191-200, 2013.
[2] X. Perpina, JF. Serviere, J. Urresti-Ibanez, I. Cortés, X. Jorda, S. Hidalgo, J. Rebollo, M. Mermet-Guyennet, "Analysis of Clamped Inductive Turnoff Failure in Railway Traction IGBT Power Modules Under Overload Conditions", *IEEE Trans. Ind. Electron.*, vol/issue: 58(7), pp. 2706–2714, 2011.
[3] M. Honsberg, T. Radke, "3-Level IGBT Modules With Trench Gate IGBT and Their Thermal Analysis in UPS, PFC and PV Operation Modes," in 13th European Conference on Power Electronics and Applications, 2009. EPE '09, pp. 1–7, 2009.
[4] X. Lu, K. Sun, Y. Ma, L. Huang, S. Igarashi, "High Performance Hybrid Cascaded Inverter for Renewable Energy System", in 2011 Twenty-Sixth Annual IEEE Applied Power Electronics Conference and Exposition (APEC), pp. 970–975, 2011.
[5] P. Petit, M. Aillerie, TV. Nguyen, JP. Charles, "Basic MOSFET Based vs Couple-coils Boost Converters for Photovoltaic Generators", *Int. J. Power Electron. Drive Syst. IJPEDS*, vol/issue: 4(1), pp. 1–11, 2014.
[6] C. Batunlu, A. Albarbar, "A Technique for Mitigating Thermal Stress and Extending Life Cycle of Power Electronic Converters Used for Wind Turbines", *Electronics*, vol/issue: 4(4), pp. 947–968, 2015.
[7] D. Dujic, GK. Steinke, M. Bellini, M. Rahimo, L. Storasta, JK. Steinke, "Characterization of 6.5 kV IGBTs for High-Power Medium-Frequency Soft-Switched Applications", *IEEE Trans. Power Electron*, vol/issue: 29(2), pp. 906–919, 2014.
[8] H. Arabshahi, "A Study of Gate Length and Source-Drain Bias on Electron Transport Properties in SiC Based MOSFETs Using Monte Carlo Method", *Int. J. Electr. Comput. Eng. IJECE*, vol/issue: 1(1), pp. 17–20, 2011.
[9] K. Shirabe, MM. Swamy, JK. Kang, M. Hisatsune, Y. Wu, D. Kebort, J. Honea, "Efficiency Comparison Between Si-IGBT-Based Drive and GaN-Based Drive", *IEEE Trans. Ind. Appl.*, vol/issue: 50(1), pp. 566–572, 2014.
[10] M. Imaizumi, N. Miura, "Characteristics of 600, 1200, and 3300 V Planar SiC-MOSFETs for Energy Conversion Applications", *IEEE Trans. Electron Devices*, vol/issue: 62(2), pp. 390–395, 2015.
[11] MC. Lee, AQ. Huang, "An Injection Efficiency Model to Characterize the Injection Capability and Turn-Off Speed For >10 Kv 4H-Sic Igbts", *Solid-State Electron*, vol. 93, pp. 27–39, 2014.
[12] I. Pesic, D. Navarro, M. Miyake, M. Miura-Mattausch, "Degradation Of 4H-Sic IGBT Threshold Characteristics Due To Sic/Sio2 Interface Defects", *Solid-State Electron*, vol. 101, pp. 126–130, 2014.
[13] M. Swamy, K. Shirabe, J. Kang, "Power Loss, System Efficiency, and Leakage Current Comparison between Si IGBT VFD and SiC FET VFD With Various Filtering Options", *IEEE Trans. Ind. Appl.*, vol/issue: PP(99), pp. 1–1, 2015.
[14] C. Codreanu, M. Avram, E. Carbunescu, E. Iliescu, "Comparison of 3C–SiC, 6H–SiC and 4H–SiC MESFETs Performances", *Mater. Sci. Semicond. Process.*, vol/issue: 3(1–2), pp. 137–142, 2000.
[15] G. Deboy, H. Hulsken, H. Mitlehner, R. Rupp, "A Comparison Of Modern Power Device Concepts for High Voltage Applications: Field Stop-IGBT, Compensation Devices And Sic Devices", in Bipolar/BiCMOS Circuits and Technology Meeting, 2000. Proceedings of the 2000, pp. 134–141, 2000.
[16] "Online Materials Information Resource", 2011. Available: http://www.matweb.com/. [Accessed: 15-Jul-2014].
[17] M. Riccio, L. Maresca, A. Irace, G. Breglio, Y. Iwahashi, "Impact of Gate Drive Voltage on Avalanche Robustness of Trench Igbts", *Microelectron. Reliab.*, vol/issue: 54(9–10), pp. 1828–1832, 2014.
[18] X. Perpiñà, X. Jordà, J. León, M. Vellvehi, D. Antón, S. Llorente, "Comparison of Temperature Limits for Trench Silicon IGBT Technologies for Medium Power Applications", *Microelectron. Reliab.*, vol/issue: 54(9–10), pp. 1839–1844, 2014.
[19] LM. Selgi, L. Fragapane, "Experimental Evaluation of A 600 V Super-Junction Planar PT IGBT Prototype #X2014; Comparison with Planar PT and Trench Gate PT Technologies", in 2013 15th European Conference on Power Electronics and Applications (EPE), pp. 1–7, 2013.
[20] M. Zerarka, P. Austin, M. Bafleur, "Comparative Study of Sensitive Volume and Triggering Criteria Of SEB in 600 V Planar and Trench Igbts", *Microelectron. Reliab.*, vol/issue: 51(9–11), pp. 1990–1994, 2011.
[21] M. Tanaka, I. Omura, "Structure Oriented Compact Model for Advanced Trench IGBTS Without Fitting Parameters for Extreme Condition: Part I", *Microelectron. Reliab.*, vol/issue: 51(9–11), pp. 1933–1937, 2011.
[22] N. Luther-King, EMS. Narayanan, L. Coulbeck, A. Crane, R. Dudley, "Comparison of Trench Gate IGBT and CIGBT Devices for Increasing the Power Density From High Power Modules", *IEEE Trans. Power Electron.*, vol/issue: 25(3), pp. 583–591, 2010.

[23] N. Luther-King, EMS. Narayanan, L. Coulbeck, A. Crane, R. Dudley, "Comparison of Trench Gate IGBT and CIGBT Devices for 3.3kv High Power Module Applications", in 2010 International Symposium on Power Electronics Electrical Drives Automation and Motion (SPEEDAM), pp. 545–549, 2010.

[24] N. Patil, D. Das, M. Pecht, "A Prognostic Approach for Non-Punch Through and Field Stop IGBTs", *Microelectron. Reliab.*, vol/issue: 52(3), pp. 482–488, 2012.

[25] X. Kang, A. Caiafa, E. Santi, JL. Hudgins, PR. Palmer, "Characterization and Modeling of High-Voltage Field-Stop IGBTS", *IEEE Trans. Ind. Appl.*, vol/issue: 39(4), pp. 922–928, 2003.

[26] AJ. Forsyth, SY. Yang, PA. Mawby, P. Igic, "Measurement and Modelling of Power Electronic Devices at Cryogenic Temperatures", Circuits Devices Syst. IEE Proc., vol/issue: 153(5), pp. 407–415, 2006.

[27] M. Bakran, HG. Eckel, M. Helsper, A. Nagel, "Challenges in Using the Latest Generation of IGBTs in Traction Converters", presented at the EPE Journal, 2005.

[28] W. Choi, D. Son, M. Hallenberger, "Driving and Layout Design for Fast Switching. Super-Junction MOSFETs", 26-Nov-2014.

[29] L. Dupont, Y. Avenas, PO. Jeannin, "Comparison of Junction Temperature Evaluations in a Power IGBT Module Using an IR Camera and Three Thermosensitive Electrical Parameters", *IEEE Trans. Ind. Appl.*, vol/issue: 49(4), pp. 1599–1608, 2013.

[30] N. Patil, D. Das, M. Pecht, "Anomaly Detection for IGBTS Using Mahalanobis Distance", *Microelectron. Reliab.*, vol/issue: 55(7), pp. 1054–1059, 2015.

[31] A. Caiafa, A. Snezhko, JL. Hudgins, E. Santi, R. Prozorov, "IGBT Operation at Cryogenic Temperatures: Non-Punch-Through and Punch-Through Comparison", in Power Electronics Specialists Conference, 2004. PESC 04. 2004 IEEE 35th Annual, vol. 4, pp. 2960–2966, 2004.

[32] M. Tounsi, A. Oukaour, B. Tala-Ighil, H. Gualous, B. Boudart, D. Aissani, "Characterization of High-Voltage IGBT Module Degradations under PWM Power Cycling Test at High Ambient Temperature", *Microelectron. Reliab.*, vol/issue: 50(9–11), pp. 1810–1814, 2010.

[33] F. Musavi, M. Edington, W. Eberle, WG. Dunford, "Control Loop Design for a PFC Boost Converter With Ripple Steering", *IEEE Trans. Ind. Appl.*, vol/issue: 49(1), pp. 118–126, 2013.

[34] SS. Saha, "Efficient Soft-Switched Boost Converter for Fuel Cell Applications", *Int. J. Hydrog. Energy*, vol/issue: 36(2), pp. 1710–1719, 2011.

[35] T. Haripriya, AM. Parimi, UM. Rao, "Modeling of DC-DC Boost Converter using Fuzzy Logic Controller for Solar Energy System Applications", in Microelectronics and Electronics (PrimeAsia), 2013 IEEE Asia Pacific Conference on Postgraduate Research in, pp. 147–152, 2013.

[36] S. Tammaruckwattana, K. Ohyama, "Experimental Verification Of Variable Speed Wind Power Generation System using Permanent Magnet Synchronous Generator by Boost Converter Circuit", in IECON 2013 - 39th Annual Conference of the IEEE Industrial Electronics Society, pp. 7157–7162, 2013.

[37] T. Kim, M. Jang, VG. Agelidis, "Practical Implementation of a Silicon Carbide-Based 300 kHz, 1.2 kW Hard-Switching Boost-Converter and Comparative Thermal Performance Evaluation", *IET Power Electron*, vol/issue: 8(3), pp. 333–341, 2015.

[38] B. Wrzecionko, S. Kach, D. Bortis, J. Biela, JW. Kolar, "Novel AC Coupled Gate Driver for Ultrafast Switching of Normally-off SiC JFETs", in IECON 2010 - 36th Annual Conference on IEEE Industrial Electronics Society, pp. 605–612, 2010.

BIOGRAPHIES OF AUTHORS

C. Batunlu is a graduate teaching assistant and is in his final year of Ph.D. After obtaining a first class degree in Electrical and Electronic Engineering from Eastern Mediterranean University in 2011, he studied Electrical Engineering and Renewable System Engineering at University of Leeds and was awarded his M.Sc. in 2013.

A. Albarbar is a Reader in Mechanical Engineering with School of Engineering, Manchester Metropolitan University. He has been working for 25 years (with both industry and academia) in which he led/participated in a number of successful major research and development projects. To date, he supervised to completion 11 PhD and more than 17 other research degrees and published over 70 articles. Alhussein studied Electronic Instrumentation Systems at UMIST and Mechanical Engineering at the University of Manchester. His main field of research is power plants design; control/monitoring strategies and reliability analysis.